

Performance Enhancement of UWB Power Control Using Ranging and Narrowband Interference Mitigation Technique

Rashid Saeed¹, Sabira Khatun², Borhanuddin Ali³, and Mohamad Abdullah²

¹Telekom Malaysia, Research and Development Innovation Centre, Malaysia

²Department of Computer and Communications Engineering, University Putra Malaysia, Malaysia

Abstract: Power control is a critical parameter for the design and evaluation of UWB-based WPAN networks due to its distributed control nature and non-fixed topology. The main issues in UWB PC are the channel gain fluctuations induced by indoor channel fluctuation and interference arising from narrowband systems. In this paper we introduce a joint PHY/MAC technique for DS-UWB power control design by exploiting the high time resolution of the UWB signal for channel gain improvement and mitigate the narrowband interference to reduce transmitted power. The results indicate that the proposed approach achieves better BER and throughput over previous works.

Keywords: Ultra-wideband, power control, narrowband interference, NBI, TOA.

Received July 9, 2007; accepted December 24, 2007

1. Introduction

Ultra-WideBand (UWB) Technology will play a key role in short range wireless connectivity. This is due to the potential advantages of UWB transmissions such as low power consumption, very high data rate, immunity to multipath fading, less complex transceiver hardware, and location capabilities. Ultra-wideband as a physical layer technique brings many features to the network. Interest in UWB is motivated by features due to extremely wide bandwidth (several GHz); potential for significant multipath capture, fine time resolution, high data rate, and low power transmission. These features also bring several challenges to UWB physical layer and upper layers design, for instance the need for the receiver to have a long acquisition time due to the very short pulse, the need to operate with a dynamic interference profile from other spectrum users (narrowband systems) as well as UWB network users, arising from the large bandwidth UWB physical layer in the network and during the transmission, the MAC layer needs to reconfigure the Power Control (PC) from time to time due to channel gain variation, wireless channel fluctuation, and nodes mobility. For robust PC design, ranging between nodes should be performed for adaptive channel gain estimation [12]. UWB suffers from Narrow Band Interference (NBI) due to the large bandwidth that UWB spreads over. PC is considered as an effective way in DS-UWB based systems to combat MUI, guarantee the required SINR at the receiver. However, this is not true in Multiple Radio Interference (MRI) environments. For example, when a link experiences deep narrowband interferer, power control

significantly increases its transmission power to keep the same SINR at the receiver. This large transmission power introduces large interference to other links and reduces the system capacity [16]. So for accurate power control design, NBI should be mitigated.

In [15] the proactive and adaptive approach for rate assignment and power control problems has been examined. The paper discussed tradeoffs between throughput and range to promote fairness in the network by power control optimization. However, the effect of mobility on the protocol was not investigated, where only stationary nodes are considered.

An uncoordinated MAC protocol for UWB networks with rate adaptation and interference mitigation to improve throughput and energy consumption was presented in [13]. The impulsive interference was mitigated at the physical layer as well as at the link layer. However, the ranging capability was not used. Uncoordinated UWB tailored MAC algorithm medium access networks (UWB) 2 was described in [2] based on pure Aloha with synchronization. (UWB)2 exploited ranging capability offered by UWB PHY layer. Distance information between transmitter and receiver was collected during control packet exchange. Multi User Interference (MUI) was modelled based on packet collisions. In [3], a Dynamic Channel Coding (DCC) based protocol was extended by incorporating a model for a UWB mobile ad-hoc networks physical layer as well as new MAC layer protocols. Joint PHY/MAC layer design was developed with the idea of arranging the physical layer and the MAC protocol such that

collisions may be replaced by rate reduction. Due to the advantages of pulsed TH-UWB, it has been adopted to come out with an interference mitigation scheme that reduces the impact of strong interferers.

In this paper we introduce a joint PHY/MAC design for DS-UWB power control design by exploiting the high time resolution of the UWB signal for high ranging estimation accuracy using Time-Of-Arrival (TOA) algorithm for Non-Line-Of-Sight (NLOS) environments and mitigate the narrowband interference to reduce transmitted power using doublet Gaussian pulse shape. The rest of the paper is organized as follows. In section 2, the UWB signal model is presented; section 3 discusses the power control design evaluation. Sections 4 and 5 present ranging estimation and narrowband interference analysis and mitigation; respectively. Simulation numerical results and discussions are discussed in section 6. Finally, section 7 concludes the paper.

2. UWB Signal Model

A Gaussian doublet is comprised of a pair of separated 2nd Gaussian's monocycle, a positive pulse followed by a negative pulse. This offers two degrees of freedom, time separation between the two pulses in the doublet and time separation between doublets.

$$p(t) = p_0(t) - p_1(t) \tag{1}$$

The 2nd Gaussian derivative $p_{G2}(t)$ can be expressed as:

$$p_{G2}(t) = -A_{G2} \frac{1 - (t - \mu)^2 / \sigma^2}{\sqrt{2\pi}\sigma^2} \exp\left(-\frac{(t - \mu)^2}{2\sigma^2}\right) \tag{2}$$

where the parameter σ determines the monocycle width T_p . The effective time duration of the waveform that contains 99.99% of the total monocycle energy is $T_p = 7\sigma$ centered on $\mu = 3.5\sigma$. The factor A_{G2} is introduced so that the total energy of the monocycle is normalized to unity, i.e., $\int p_{G2}^2(t) dt = 1$. With spectrum analysis of equation 2 the (ESD):

$$|P(\omega)|^2 = 4\pi e. (\omega t_p^2)^2 . e^{-(\omega t_p)^2} . [1 - \cos \omega T_n] \tag{3}$$

Since $\omega = 2\pi f$, the null frequencies in ESD are, $\pi(2fT_n) = 0, 2\pi, \dots, 2k\pi$, then $f = (k/T_n)$, where $k=1, 2, \dots$. Using equations 1, 2 and 3, the doublet Gaussian pulse in time domain and frequency domain are shown in Figures 1 and 2, respectively.

The null frequencies of Gaussian doublet in Figure 2 can be controlled by regulating the position of the second Gaussian pulse (the first pulse $p_0(t)$ begins at $t = 0$, the second one $p_1(t)$ begins at $t = T_n$). From the figure we can see that the PSD is skewed. As depicted

in Figure 2 there notch spectral in the doublet waveform which can be used to mitigate interference from other systems.

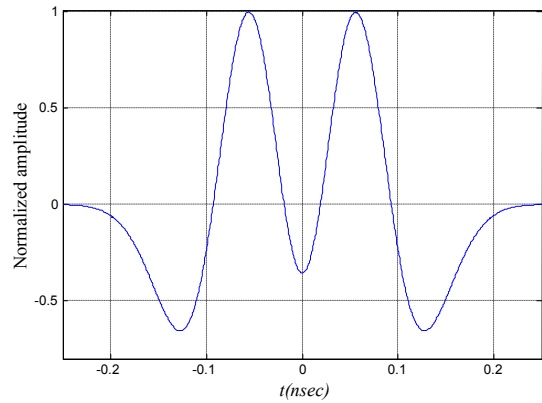


Figure 1. Time-domain representation for Gaussian doublet pulse with time delay between the pulses $T_n = 0.1n$ sec.

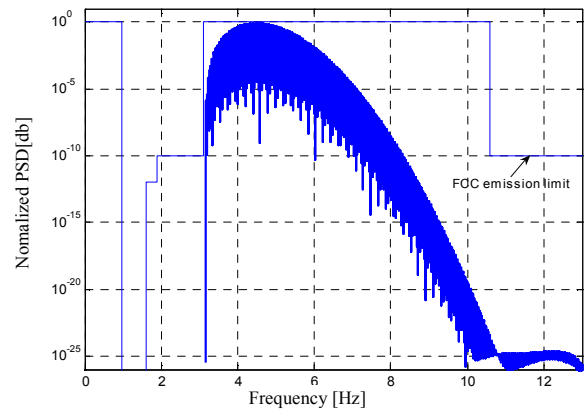


Figure 2. Power spectral density of doublet Gaussian pulse and FCC emission limit for indoor systems.

3. Power Control Design

Power control is the process of determining the transmitted power of each communication terminal in the UWB network. Adjusting the transmitted power is extremely important for UWB ad-hoc networks because the transmitting node needs to sense the Signal-to-Interference and Noise-Ratio (SINR) at receiving node [10]. If the SINR is lower than the target value then the transmitting node increases its transmitted power and vice versa so as to improve the total system performance.

A measure of the link quality (related to bit error rates) is the SINR observed at the receiver [11]. Indeed the link throughput is an increasing function of the SINR. Thus, the link power control is an increasing function of the SINR overall. To simplify the discussion, we base our formulation of the power control problem directly on the SINR and consider the above problems of mobility and NBI. Let

$$SINR = \frac{P_{ij}(t)g_{ij}(t)}{\sigma_{rec}^2 + \sum_{k=1, k \neq i, j}^Q P_k g_{kj}(t) + \sigma_{bm}^2 |_{m \in I_j}} \tag{4}$$

where σ_{rec}^2 is the noise power, $P_{ij}(t)$ and $g_{ij}(t)$ are the power and channel gain between node i to node j , respectively, $i, j \in \{1, 2, 3, \dots, N\}$, and $\sigma_{bm}^2 |_{m \in I_j}$ is the narrowband interference which affects the quality of the radio link, producing more packet losses, and result in an overall rate reduction and an increased energy consumption. Interference has a large impact on the system performance and needs to be taken into account as early as in the design phase. $g_{ij}(t)$ is modelled as a combination of distance $|x_i - x_j|$, path loss (α) and Rayleigh fading (multipath) channel $\Gamma(t)$ where

$$g_{ij}(t) = \frac{g_0(t)}{\sum_{k=1}^K |X_i^k - X_i^{k-1}|^\alpha / \Gamma^k(t)} \quad (5)$$

and I_j is the set of narrowband nodes that can cause interference at UWB node i ; $g_0(t)$ is a reference value for power gain evaluated at $D = 1$ m. To calculate the distance between the nodes we can write:

$$|x_i - x_j| = c \cdot \tau_{ij} \quad (6)$$

where c is the speed of light and τ_{ij} is the estimated time of received signal at node j , given by [10]:

$$\tau_{ij} = \tau_{TOA} + \varepsilon \quad (7)$$

where τ_{TOA} is the time-of-arrival and ε is the time offset obtained from mean acquisition time, which is the time the receiver need to synchronize with the transmitter for more accurate TOA estimation. TOA technique computes distance based on the estimation of the propagation delay between transmitter and receiver. In order to do that the maximum likelihood estimator was used as follows [6]:

$$\hat{\tau}_{TOA(ML)}(r) = \arg \min_{\tau \in \mathbb{R}} \left(e^{-\frac{1}{N_0 T_{obs}} \int (r(t) - s(t - \tau_d))^2 dt} \right) \quad (8)$$

where N_0 is the Power Spectral Density (PSD) of the noise and T_{obs} is the observation interval over which the estimation is performed. We can write that, for each link i there is a lower SINR threshold γ_i^T , reflecting a certain QoS the link has to maintain in order to operate properly [8]. Therefore, we require that:

$$SINR = \frac{P_{ij}(t)g_{ij}(t)}{\sigma_{rec}^2 + \sum_{k=1, k \neq i, j}^Q P_k g_{kj}(t) + \sigma_{bm}^2 |_{m \in I_j}} \geq \gamma_i^T(t) \quad (9)$$

for every $i, j \in \{1, 2, 3, \dots, N\}$. The term $\sum_{k=1, k \neq i, j}^Q P_k g_{kj}(t)$

is known as MUI, where in DS-UWB, each code has the effect of modifying the transmitted signal in such a way that a reference receiver is capable of isolating the useful signal from other users' signals, which are seen as interfering signals to the receiver. The possibility of removing this undesired interference mainly depends on the characteristics of the codes used for separating data flows, and on the degree of system-level synchronization. In realistic scenarios devices do not achieve ideal synchronization and codes lose orthogonality due to different propagation delays on different paths, the receiver might not be capable of completely removing the presence of the undesired signals, and as a consequence, system performance is affected by MUI. A detailed analysis of MUI has been discussed extensively in [8].

UWB communication system parameters (such as the number of users, bit rates and achieved SINR) represent the resources made available by the UWB physical layer (such as pulse shape, bandwidth, processing gain, and number of pulses per bit). By adjusting these system parameters, it is possible to design a high throughput MAC protocol for UWB. The wide range of values of the UWB parameters enables the design of highly adaptive PHY/MAC design which may be matched to a wide range of service requirements [6]. In addition to focusing on the resources to be managed, possible constraints imposed by the UWB technology itself must be taken into account. In the next section we will discuss ranging estimation between nodes and narrowband interference mitigation for more robust power control design.

4. Ranging Design

The fine time resolution of UWB signals enables potential applications in high-resolution of channel gain adaptation. The novel aspect of UWB TOA is that the multipath time-spread in many channels of interest is often 100 to 1000 times the inherent time resolution of the UWB signal detected in a matched filter receiver. Some of the parameters that have been traditionally used for distance calculation are the Received Signal Strength Intensity (RSSI), the Angle Of Arrival (AOA) and TOA [6].

Amongst these parameters, RSSI is the least adequate in the case of UWB because of the cumulative impulsive signals strength due to multipath and requires a site-specific path loss model [17]. The estimation of AOA, on the other hand, requires multiple antennas (or at least an antenna capable of beam forming) at the receiver. This requirement implies size and complexity demands that are often not compatible with the low-cost, small-size

constraints associated with applications such as wireless sensor networks, which UWB technology is particularly suited for. Given a transmitted signal $s(t)$, the corresponding received signal can be written as:

$$r(t) = h(t) * s(t) + n(t) \tag{10}$$

where $h(t)$ is the channel impulse response and $n(t)$ is AWG noise. If the signal propagates over a perfect channel the impulse response can be written as:

$$h(t) = A(d)\delta(t - \tau(d)) \tag{11}$$

where d is the distance between the transmitter and the receiver. The received signal can be written as:

$$r(t) = A(d)s(t - \tau(d)) + n(t) \tag{12}$$

Equation 12 indicates that distance d can be estimated from either attenuation $A(d)$ or delay $\tau(d)$. The use of $A(d)$ versus $\tau(d)$ determines the method for estimating distance; Received Signal Strength Intensity (RSSI) versus TOA, respectively. The TOA technique computes distance based on the estimation of the propagation delay between transmitter and receiver. TOA is the most commonly used distance estimation method in the radar field.

Assume that a single UWB pulse is transmitted over a multipath channel, then the received signal can be expressed as the sum of the first signal path, other multipath components and noise:

$$r(t) = \alpha_1 p(t - \tau_1) + \sum_{l=2}^L \alpha_l p(t - \tau_l) + n(t) \tag{13}$$

where $\tau_1 < \tau_2 < \dots < \tau_L$. L is the number of multipaths, where L are unknown. We also assume that the delay and channel coefficient for the strongest multipath component, τ and α , are determined beforehand by means of a correlation technique; for example, they can be estimated by exhaustively searching possible delay positions, and choosing the one with maximum correlation output [8]. A two-step algorithm as in [7], can be employed first to obtain a rough estimate of the signal delays and then to seek the strongest component in the block. Then, consider the signal components including and prior to the strongest path and truncating the $\tilde{r}(t)$ to $t \leq T_p/2$, we can write :

$$\begin{aligned} \tilde{r}(t) &= \bar{r}(t), & t &\leq \frac{T_p}{2} \\ \tilde{r}(t) &= \tilde{\alpha}_1 p(t + \tilde{\tau}_1) + \sum_{l=2}^M \tilde{\alpha}_l p(t + \tilde{\tau}_l) + \tilde{n}(t) \end{aligned} \tag{14}$$

where T_p is the doublet Gaussian pulse width $p(t)$, M is the number of multipath components before the strongest component. If $M = 0$, then $\tilde{\tau}_1 = 0$, $\tilde{\alpha}_1 = \pm 1$,

and the second term in equation (14) is ignored. $\tilde{n}(t)$ is white Gaussian noise truncated to the time interval $(-\infty, T_p/2]$ [14]. After wide-band filtering and sampling $\tilde{r}(t)$, we can write the vector \tilde{r} as:

$$\tilde{r} = \tilde{\alpha}_1 p_{\tilde{\tau}_1} + \sum_{l=2}^M \tilde{\alpha}_l p_{\tilde{\tau}_l} + \tilde{n} \tag{15}$$

where $p_{\tilde{\tau}_1}$ is a vector consisting samples from $p(t + \tilde{\tau}_1)$ with the same length of \tilde{r} . Since \tilde{n} is a white Gaussian vector, then we can write the estimate $\tilde{\tau}_1$ as:

$$\hat{\tilde{\tau}}_1 = \arg \max_{\tilde{\tau}_1} \left[\min_{\tilde{\alpha}_1, M, \tilde{\alpha}, \tilde{\tau}} \left\| \tilde{r} - \tilde{\alpha}_1 p_{\tilde{\tau}_1} - \sum_{l=2}^M \tilde{\alpha}_l p_{\tilde{\tau}_l} \right\|^2 \right] \tag{16}$$

where $\tilde{\alpha} = [\tilde{\alpha}_2 \dots \tilde{\alpha}_M]$ and $\tilde{\tau} = [\tilde{\tau}_2 \dots \tilde{\tau}_M]$. The computation of TOA estimation by equation 16 was evaluated by using the iteration in Figure 3 coded by MATLAB® 7.4. The thresholds of the algorithm, $\theta_{\tilde{\tau}_1}$ and $\theta_{\tilde{\alpha}_1}$, are important thresholds that determine the performance of the estimator. Therefore, those critical thresholds can be selected based on some statistical information obtained from channel impulse response in specific environment [18].

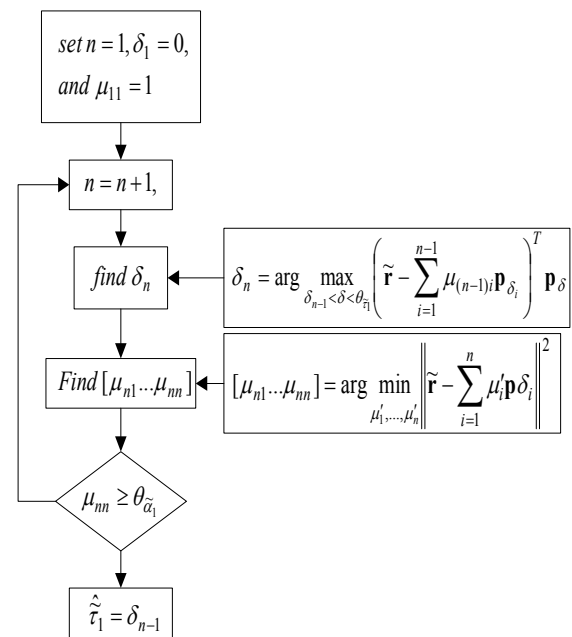


Figure 3. Time-of-arrival estimation algorithm flow chart.

5. Interference Analysis and Mitigation

UWB systems are able to co-exist with narrowband technologies due to regulation by FCC in Feb. 2002, as shown in Figure 2. However, conversely the influence of narrowband signals on the UWB system can be significant, and in the extreme case, these signals may jam the UWB receiver completely [8]. Even though narrowband signals interfere with only a small fraction of the UWB spectrum, due to their

relatively high power with respect to the UWB signal, the performance and capacity of UWB systems can be affected considerably. Recent studies show that the BER performance of the UWB receivers is greatly degraded due to the impact of NBI [16] as shown in Figure 4.

Consider the presence of narrowband interferer signal within the DS-UWB system. Then the signal at the receiver can be written as:

$$r(t) = \sum_{k=1}^{N_u} \sqrt{A_k E_c^{(k)}} \sum_i b_i^{(k)} \sum_{l=0}^{N_c-1} c_l^{(k)} h^{(k)}(t) * p(t - lT_c - iT_f) + n(t) + \sigma_b^2 \quad (17)$$

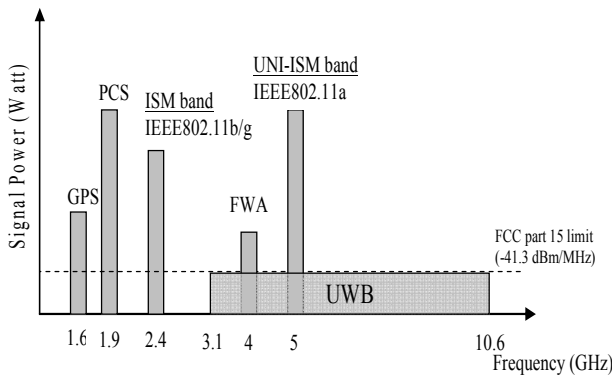


Figure 4. Spectrum crossover of the narrowband interferers in UWB systems.

where N_u is number of users, A_k represent the attenuations due to pass loss, $E_c^{(k)}$ is the energy per transmitted pulse for user k . This is modelled with doublet Gaussian pulse $p(t)$. $n(t)$ is the Gaussian process with two sided power spectral density $N_0/2$ and $\sigma_b^2 = \sqrt{A_b} n_b(t)$ is the variance of narrowband interference, $n_b(t)$ is the narrowband interference, $h^k(t)$ is the time-invariant asynchronous multipath channel impulse response for user k . ‘*’ denotes convolution, and A_k, A_b represent the attenuations due to path loss, which are functions of the transmitter-receiver distance. In order to evaluate the narrowband interference analytically, we construct a discrete time equivalent model of the narrowband interference by sampling $n_b(t)$ every T_s seconds, with $T_s \ll T_c$. The vector containing the discrete sample is given as:

$$\vec{n}_b = [n_b(0), n_b(T_s), \dots, n_b((N_w - 1)T_s)]^T, \vec{n}_b \in \mathfrak{R} \quad (18)$$

where T_s is the sampling time, $N_w = T_w/T_s$ is the number of samples in observation window T_w over which the receiver operates. The power spectral density of the narrowband interference can be written as:

$$S_{nb}(f) = \begin{cases} N_b/2, & f_I - B_b/2 \leq |f| \leq f_I + B_b/2 \\ 0, & \text{otherwise} \end{cases} \quad (19)$$

where f_I and B_b are the central frequency and bandwidth of the narrowband interference, respectively, and $N_b/2$ is the Power Spectral Density (PSD) of the interference within its bandwidth. We consider two types of In-Band Interference (IBI); an IEEE802.11a system with central frequency $f_I = 5.3$ GHz, and bandwidth $B_b = 200$ MHz, fixed Wireless Access (FWA) network with central frequency $f_I = 3.9$ GHz and bandwidth $B_b = 160$ MHz [16]. The autocorrelation function of $n_b(t)$ is therefore given by:

$$R_b(\tau) = \frac{N_b}{2} \tilde{R}_b(\tau) \quad (20)$$

where $\tilde{R}_b(\tau) = 2B_b \cos(2\pi f_I \tau) \text{sinc}(\pi B_b \tau)$, and we can evaluate NBI variance as:

$$\sigma_b^2 = A_b \frac{N_b}{2} |\tilde{R}_b| \quad (21)$$

Pulse shaping is an emerging approach for a more efficient usage of the precious radio spectrum resources and to fit to FCC spectrum mask. It considers an expanded view of the wireless channel by managing and adapting pulse parameter dimensions of time, frequency, space, power, and coding. In the next section, we will discuss pulse shaping in order to self-adapt the UWB pulse parameters and minimize in-band narrowband interference typically; WLAN and FWA.

5.1. Pulse Shaping for Spectrum Adaptation

In the analysis herein, we assume an All Rake (ARake) receiver, which consists of multiple correlators employing the template signal of $v(t) = p(t) - p(t - \tau_k)$, τ_k is the excess delay of the k^{th} path. When appropriately synchronized and assuming the pulse shape $p(t)$ known to the receiver, the correlation output over a symbol interval of the k^{th} path, denoted by r_k ($k = 1, 2, \dots, N_r$), is given by:

$$r_k = \hat{b}_i^{(k)} s_k + n_{b_k} + n_k \quad (22)$$

where $\hat{b}_i^{(k)}$ is estimated at detector, and s_k, n_{b_k}, n_k are the symbol interval of the k^{th} path for the transmitted signal, narrowband interference signal, and AWGN signal, respectively.

$$\begin{aligned} s_k &= AN_s \int_{-\infty}^{\infty} p_r(t) [p_r(t) - p_r(t - \tau_k)] \\ &= AN_s m_p(\delta) \end{aligned} \quad (23)$$

$$n_{b_k} = \sum_{i=0}^{N_c-1} \int_{-\infty}^{\infty} i(t + iT_f + c_i T_c) v(t) dt \quad (24)$$

$$n_k = \sum_{i=0}^{N_c-1} \int_{-\infty}^{\infty} n(t + iT_f + c_i T_c) v(t) dt \quad (25)$$

The correlation matrix of the interference samples $R_{n_b} = E \left\{ \begin{matrix} n_{b_k} \\ n_{b_l} \end{matrix} \right\}^*$ are collected over a symbol interval at different paths. Since the UWB spectrum will be basically constant over the frequency range of NBI centered at f_I [4], then (k, l) element of R_{n_b} can be derived as:

$$[R_{n_b}]_{k,l} = N_s |P_r(f_I)|^2 [2R_{n_b}(0) - R_{n_b}(\varepsilon_k) - R_{n_b}(\varepsilon_l)] \quad (26)$$

where $|P_r(f_I)|^2$ is the power spectral density of the received pulse $p_r(t)$ at the frequency f_I . We can conclude that the effect of NBI on UWB systems is maximum when the NBI center frequency overlaps with nominal center frequency of UWB spectrum. To mitigate the presence of narrowband interference in UWB receiver a notch filter should be placed after the ARake to filter out the interference part around f_I ($|P_r(f_I)|^2 = 0$) from the pulse power spectrum $|P_r(f)|^2$. Then we can write the transfer function of the notch filter as:

$$H(f) = 1 - \left[u\left(f - f_I + \frac{B_b}{2}\right) - u\left(f - f_I - \frac{B_b}{2}\right) \right] \quad (27)$$

and impulse response as:

$$h(t) = \delta(t) - B_b e^{j2\pi f_I t} \sin c(B_b t) \quad (28)$$

where B_b represents the width of the spectral notch, which is set to be sufficiently larger than the bandwidth of the narrowband interference. This can be performed by a filter bank [8]. Having notched out the interference, the remaining signal is restored to the time domain by performing inverse fourier transform, which can be expressed as:

$$\tilde{r}(t) = A b_i p_{notch}(t - iT_f - c_i T_c) + n(t) \quad (29)$$

$$p_{notch}(t) = p_r(t) - P_r(f_I) B_b e^{j2\pi f_I t} \sin c(B_b t) \quad (30)$$

where t is in nanosecond and B_b is in gigahertz. For suppression of typical NBI, $B_b \ll 1$; moreover, due to the low power of UWB transmission system, $P_r(f_I)$ is also of a small value. So the notched pulse is expected to be only slightly different from $p_r(t)$. The rest of the signal processing takes place in time domain.

6. Simulation Results and Discussion

MATLAB® 7.4 was used to simulate and analyze the system performance in this paper.

Table 1. Simulation parameters.

Parameter	Value
Number of pulses per bit (N_p)	10
Frame duration (T_f)	2ns
Bit time (T_b)	20ns
Number of chips per bit (N_c)	10
Chips duration (T_c)	2ns
sampling interval (T_s)	0.5ns
Shaping factor for the pulse (σ)	0.25ns
Pulse width (T_p)	0.5ns
Time delay between the pulses in doublet (T_n)	0.1ns
Path attenuation exponent (α) for LOS	1.7
Path attenuation exponent (α) for NLOS	3.5

Figure 5 shows the ranging estimation error for NLOS environments versus E_b/N_0 with doublet Gaussian pulse width $T_p = 0.5ns$ and various search regions and relative strength thresholds. Results showed that in NLOS, selection of suitable thresholds leads to better ranging performance. For instance, in dense multipath NLOS it is better for the receiver to select high search region threshold and low relative strength threshold due to the higher probability of direct-path detection at these values. However, higher E_b/N_0 transmission with lower thresholds still gives good performance.

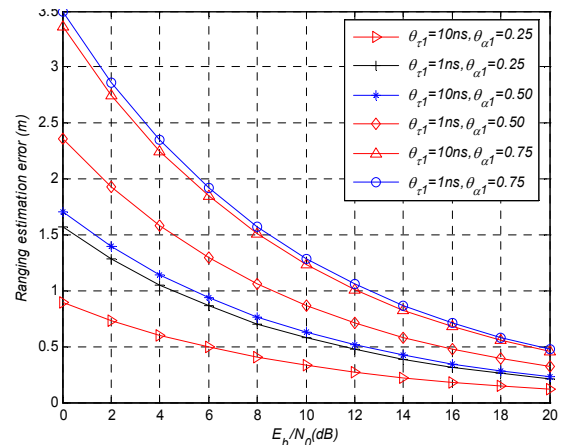


Figure 5. Ranging estimation error for NLOS channel versus E_b/N_0 with pulse width $T_p = 0.5ns$ and various search region and relative strength thresholds.

The results in Figure 6 with $\theta_{r1} = 10ns$ and $\theta_{\alpha1} = 0.25$ was compared with [9] for 2D indoor positioning technique suitable for impulse radio networks in multipath environment. Since the receivers in [9] are expected to record times only and is insensitive to amplitude or phase with given

Channel Impulse Response (CIRs), it gives low estimation error at lower SNR. However, an accurate propagation model is required to estimate distance reliably, which is very difficult in indoor environment due to nodes mobility and variations of channel behaviour, since Cramer-Rao Lower Bound (CRLB) does not give solutions for low power NLOS environments, CRLB contributes high ranging estimation error [14]. The proposed algorithm outperforms the NLOS Generalized Maximum Likelihood (NLOS-GML) [18].

Figure 7 shows the frequency domain of the proposed pulse shape with notches in the victim frequencies which is performed by randomizing the polarity of the transmitted pulses and then shifting and adjusting the center frequency of the doublet pulse. Narrowband interference depends on three factors: carrier frequency of the NB system, distance between NB node from UWB node and on the number of NB nodes [8], where the aggregate NBI can be calculated as:

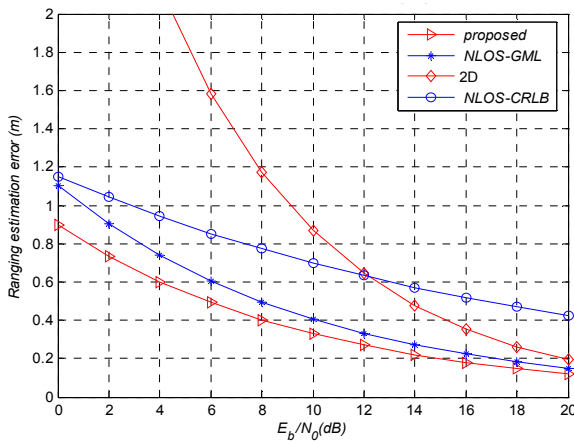


Figure 6. Ranging estimation error (REE) for NLOS with pulse width $T_p = 0.5ns$ and $\theta_{\tau_1} = 10ns$, $\theta_{\alpha_1} = 0.25$.

$$I_{agr} = \lambda \sum_m \chi_m n_b A(d_m) \quad (31)$$

Where $\lambda \leq 1$ factor describes NBI carrier frequency location from UWB center frequency, m is the number of NB nodes, and $A(d_m)$ is the overall loss between the m^{th} NB node at distance d_m from the selected UWB node. This can be solved by using Minimum Mean Square Error (MMSE) combining with low number of Rake fingers [6].

Figure 8 shows the effect of Ranging Estimation Error (REE) in power control performance. Recall the results in Figure 6, the ranging estimation error at $E_b/N_0 = 10dB$ for the proposed method is (REE=0.32m), NLOS-GML is (REE= 0.4m), 2D is (REE=0.7m), and for NLOS CRLB is (REE=0.84). From the figure the high REE leads to wrong power control calculation which leads to High Bit Error Rate (BER).

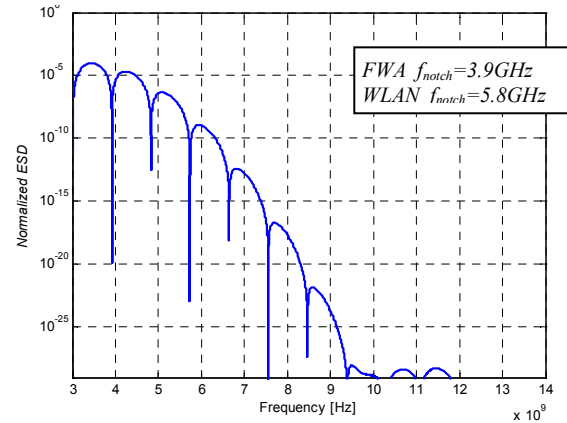


Figure 7. Normalized energy spectral density for UWB doublet Gaussian pulse to mitigate WLAN and FWA interference.

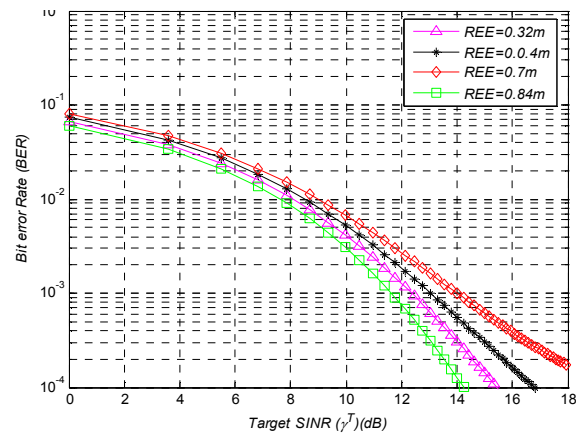


Figure 8. UWB power control performance under various REE with $N_p=10$ and $N_u=20$ nodes.

Figure 9 shows the power control performance for conventional DS-UWB, OFDM-UWB, and DS-UWB after pulse shaping. The proposed method outperforms IEEE802.15.3a proposed systems, OFDM-UWB and DS-UWB, due to interference mitigation effects.

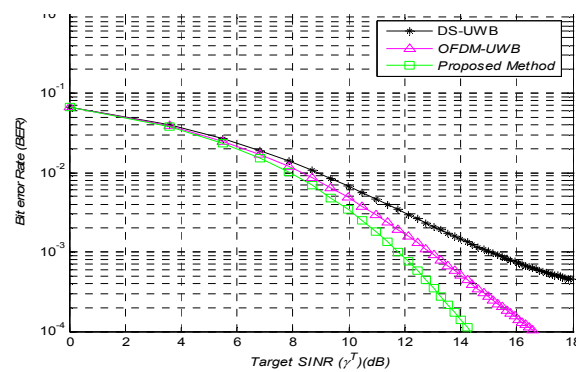


Figure 9. UWB power control performance under various UWB systems with $N_p=10$ and $N_u=20$ nodes.

Figure 10 shows the performance of UWB power control system as evaluated from equation 9 with various number of nodes (10, 20, 30, 40, and 50 nodes). For high number of users (30, 40, and 50) the BER is saturated due to increased number of packet collisions, heavy loads in the medium and MultiUser Interference (MUI). This problem can be solved by adopting space diversity that can be provided by ranging algorithm [14]. Another method to avoid

multipath interference is to lower the duty cycle of the system, and can be achieved by increasing the pulse duration (T_f), where duty cycle is given by [18]:

$$\text{duty cycle} = T_f / T_p \quad (32)$$

By transmitting pulses with time delay greater than the maximum expected multipath delay, unwanted reflections can be avoided at the receiver.

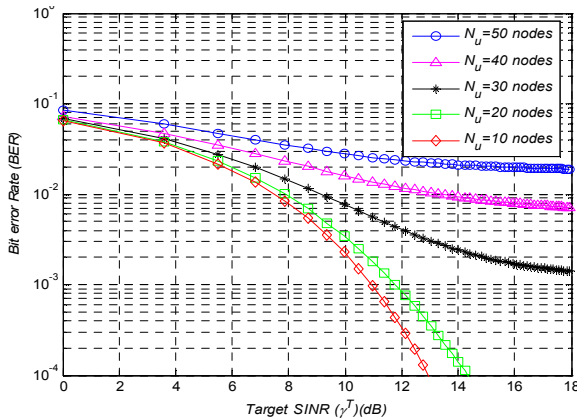


Figure 10. Proposed UWB power control performance under various numbers of nodes with $N_p=10$.

In Figure 11 various number of pulses per bit (N_p) were examined for target SINR for given bit error rates. Results show that high number of pulses per bit lead to better SINR for given BER. $N_p = 1$ means bit duration (T_b) and frame duration (T_f) are equal, which means high duty cycle equal to 1 and leads to high multipath interference, hence gives saturated curve in the figure.

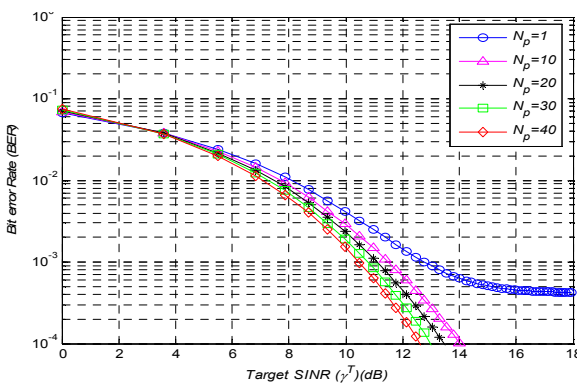


Figure 11. Proposed UWB power control performance under various numbers of pulses per bit with $N_u=20$ nodes.

In Figure 12 we compared between our proposed method and other methods from the literature. In order to emphasize the importance of an interference mitigation and ranging estimation, we compare the proposed method with DCC-MAC [3] and $(UWB)^2$ [2] protocols in term of target SINR. As seen from the figure our proposed method outperforms the other two protocols; this is because this method considers both ranging and interference mitigation. The three methods converged at low SINR values because below

SINR=5dB the dominant interference is the Multi-MUI [8].

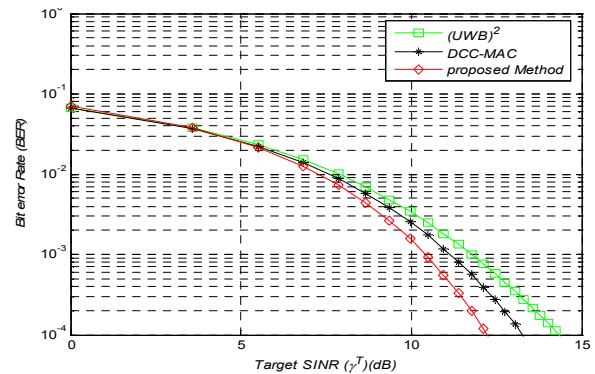


Figure 12. Comparison of BER performance of our proposed method and DCC-MAC and $(UWB)^2$ with $N_u=20$ and $N_p=10$.

Figure 13 compares the throughput between the proposed method and DCC-MAC and $(UWB)^2$. The throughput of $(UWB)^2$ decreases with the number of nodes because $(UWB)^2$ needs a common control channel for RTS-CTS handshake to access to a destination. In dense non-line-of-sight areas $(UWB)^2$ contribute large ranging estimation error. DCC-MAC outperforms $(UWB)^2$ but the performance still degraded as the number of nodes increases, compared with the proposed system.

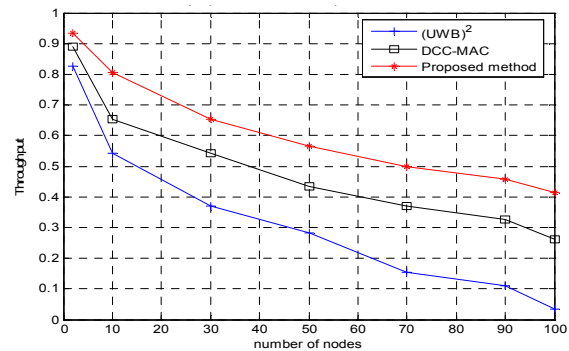


Figure 13. Performance comparison between proposed method and other related methods.

This is due to two reasons: first, because narrowband interference is combated in the MAC layer using rate adaptation, which fails with strong interferences like IEEE802.11a and IEEE802.16; second, when the number of nodes grows, nodes should depend on its local resources to avoid flooding the medium with control messages that would increase MUI.

7. Conclusion

Power control transmission is an essential MAC/PHY aspect in which accurate power control will reduce the total power consumption, implying long battery life, and controlled interference level in the network. The performance evaluation of Ultra-WideBand (UWB) power control design has been investigated. Several parameters were examined to achieve optimal power control based on ranging estimation and interference

mitigation. Ranging estimation was evaluated by time-of-arrival technique to perform the accurate timing detection. A mitigation technique using pulse shaping approach was proposed, while cognitive radio can be a topic for further studies in interference mitigation. For future work on robust and adaptive power control, more cross-layer parameters i.e., synchronization, should be considered.

References

- [1] Benedetto D. and Giancola G., *Understanding Ultra-Wideband Radio Fundamentals*, Prentice Hall, New Jersey, 2004.
- [2] Benedetto D., Nardis D., Junk M., and Giancola G., "UWB 2: Uncoordinated Wireless Baseborn, Medium Access Control for UWB Communication Networks," *Computer Journal of IEEE Mobile Networks and Applications*, vol. 3, no. 7, pp. 64-66, 2004.
- [3] Boudec L., Ruben M., and Joerg W. "A MAC Protocol for UWB Low Power Mobile Ad-Hoc Networks Based on Dynamic Channel Coding With Interference Mitigation," *Technical Report*, Switzerland, 2004.
- [4] Chu X. and Murch R., "The Effect of NBI on UWB Time Hopping Systems," *Computer Journal of IEEE Transactions on Wireless Communication*, vol. 3, no. 5, pp. 1431-1436, 2004.
- [5] Chairman M., Commissioners A., and Adelstein I., "Federal Communications Commission," *Technical Report*, the University of North Carolina, 2002.
- [6] Foerster R., "The Performance of a DS-UWB System in the Presence of Multipath, Narrowband Interference, and Multiuser Interference," in *Proceedings of the Conference on UWB Systems and Technologies*, USA, pp. 87-91, 2004.
- [7] Gezici S., Sahinoglu Z., and Poor V., "A Two Step ToA Estimation Algorithm for IR-UWB Systems," in *Proceedings of 13th European Signal Processing Conference*, Antalya, pp. 71-83, 2005.
- [8] Ghavami M., Michael L., and Kohno R., *Ultra Wideband Signals and Systems in Communication Engineering*, John Wiley and Sons, 2004.
- [9] Guo W., Filer P., and Barton K., *2D Indoor Mapping and Positioning Using an Impulse Radio Network*, Kluwer Academic Publishers, Boston, 2002.
- [10] Hayajneh M. and Abdallah T., "Statistical Learning Theory to Evaluate the Performance of Game Theoretic Power Control Algorithms for Wireless Data in Arbitrary Channels," in *Proceedings of IEEE Wireless Communication and Networking Conference*, New Orleans, pp. 723-728, 2003.
- [11] Kohno Y. and Lie R., "Optimum Multi User Detection in UWB Multiple Access Communications Systems," in *Proceedings of IEEE International Criminal Court*, UK, pp. 812-816, 2002.
- [12] Kolenchery S., Townsend J., Freebersyser J., and Bilbro G., "Performance of Local Power Control in Peer to Peer Impulse Radio Networks with Bursty Traffic," *Computer Journal of Globecom*, vol. 2, no. 1, pp. 910-916, 2000.
- [13] Manuel F., Marz R., and Le Boudec Y., "Managing Impulsive Interference in Impulse Radio UWB Networks," in *Proceedings of International Conference on Broadband Networks*, Austria, pp. 260-271, 2006.
- [14] Qi Y. and Kobayashi H., "A Unified Analysis for Cramer Rao Lower Bound for Non Line of Sight Geolocation," in *Proceedings of Information Sciences and Systems*, Spain, pp. 641-650, 2002.
- [15] Raja J., Pierre B., and Cristina L., "U-MAC: A Proactive and Adaptive UWB Medium Access Control Protocol," *Computer Journal of Wireless Communications and Mobile Computing*, vol. 5, no. 5, pp. 563-569, 2005.
- [16] Romeo G. and Franco M., "On the Coexistence of Power Controlled Ultra-Wideband Systems with UMTS and Fixed Wireless Systems," *Computer Journal of IEEE Transaction on Vehicular Technology*, vol. 45, no. 1, pp. 1-20, 2005.
- [17] Saleh A. and Valenzuela A. "A Statistical Model for Indoor Multipath Propagation," *IEEE Journal of Selected Areas in Communications*, vol. 5, no. 2, pp. 128-137, 2002.
- [18] Yong J. and Scholtz A., "Ranging in a Dense Multipath Environment Using Radio Link," *IEEE Journal on Selected Areas in Communications*, vol. 20, no. 9, pp. 763-767, 2002.



Rashid Saeed received his BSc and MSc in electronics engineering from the Sudan University of Science and Technology and Electrical Engineering, Karary Academics for Technology, Sudan in 1999 and 2001, respectively. He received his PhD from University Putra Malaysia in 2006 in computer and communications system engineering.



Borhanuddin Ali received his BSc in electrical and electronics engineering from Loughborough University of Technology in 1979, his MSc and PhD in electromagnetism engineering from the University of Wales in 1981 and 1985, respectively.



Sabira Khatun received her BSc and MSc in applied mathematics and PhD on hydromagnetic stability from the University of Rajshahi, Bangladesh in 1988, 1990 and 1994, respectively. She received her second PhD in communications and networking from University Putra Malaysia in 2003.



Mohamad Abdullah received his BSc and MSc degree in electrical engineering from University of Missouri at Rolla, USA, in 1990 and 1993, respectively, and PhD degree from University Malaya, Malaysia, in 1999.